Image Cover Sheet

CLASSIFICATION	SYSTEM NUMBER
UNCLASSIFIED	503805

TITLE

EVALUATION OF THE CAVITATION INCEPTION PREDICTION CAPABILITIES OF THE PROPELLER SURFACE PANEL CODE ASP-2

System Number:

Patron Number:

Requester:

Notes:

DSIS Use only:

Deliver to:

Evaluation of the Cavitation Inception Prediction Capabilities of the Propeller Surface Panel Code ASP-2

D. J. Noble
Defence Research Establishment Atlantic
P.O Box 1012, Dartmouth, Nova Scotia, B2Y 3Z7

ABSTRACT

This paper describes results of a comparative study performed at the Defence Research Establishment Atlantic (DREA) to evaluate the cavitation prediction capabilities of DREA's surface panel code ASP-2. This code performs an unsteady potential flow analysis of marine propellers for a specified non-uniform inflow distribution corresponding to operation in a ship's wake. ASP-2 predictions of the cavitation inception performance of two propellers designed for twin-screw surface ships are correlated with experimental data obtained both at model scale in a depressurized towing tank and on full scale sea trials. For a range of operating conditions in a ship's wake, results are presented that show a good correlation of ASP-2 predictions with experiment for cavitation forming at the leading edge of both outer radius and root sections of propeller blades. ASP-2 predictions of leading edge cavitation on the face or downstream surface of blades are also shown to be significantly closer to observations made on full scale sea trials than are model test results.

NOMENCLATURE

C_g - Unsteady depth term in total pressure coefficient
C_p - Total pressure coefficient
C_p' - Flow-dependent term in total pressure coefficient
C_p^* - Critical value of total pressure coefficient
D - Propeller diameter
g - Acceleration due to gravity
H - Depth of propeller shaft centre
J - Propeller advance coefficient
n - Propeller shaft rate in revolutions per second
n_i - Shaft revolutions per second at inception
p - Total flow pressure
p_{atm} - Atmospheric pressure at water surface
p_v - Vapour pressure of water
r - Cylindrical radial coordinate from shaft centre
t - Time variable
U - Magnitude of mean relative inflow velocity
$\vec{U}$ - Mean relative inflow velocity vector
V_a - Magnitude of mean axial inflow velocity
V_i - Ship speed at inception
V_s - Ship speed in general
V_T - Magnitude of total velocity on propeller surface
w_T - Taylor wake fraction
y_o - Upward vertical coordinate from shaft centre
ρ - Density of water
σ_n - Local cavitation number based on shaft rate
θ - Rotation plane angle from blade's spanwise axis
ϕ - Propeller-induced velocity potential
Ω - Shaft rotation rate in radians per second
$\vec{\nabla}$ - Vector gradient operator
AERCOL - Aerospace Engineering and Research Consultants Limited
ASP-1, ASP-2 - AERCOL Steady-inflow Propeller programs, versions 1 and 2
DREA - Defence Research Establishment Atlantic
MARIN - Maritime Research Institute Netherlands
MIT - Massachusetts Institute of Technology
PSF-2 - Propeller Steady Force program, version 2
PUF-10 - Propeller Unsteady Force program, version 10

INTRODUCTION

Since propeller cavitation is an important contributor to ship radiated noise, part of DREA's naval platform research involves development of computer programs for assessing the cavitation and noise performance of propellers on Canadian naval ships. Given the expense of model testing propellers, propeller analysis codes can provide a cost-effective means of optimizing the cavitation performance of new propeller designs and examining remedies to cavitation and noise problems that may arise with existing ship propellers. These codes, however, must be shown to reliably predict the cavitation performance that is observed experimentally.

The propeller surface panel code ASP-2 was developed for DREA by Canadian contractor AERCOL as an extension of the surface panel code PUF-10 developed at MIT (Hsin 1990) under U. S. Navy sponsorship. The code performs an unsteady potential flow analysis of flows generated by propellers in a rotating blade-fixed frame of reference for a specified non-uniform inflow distribution in a ship's wake that is considered steady relative to a ship-fixed reference frame.

Flow predictions obtained at blade extremities with the curved, hyperboloidal panel method used in PUF-10 were improved by AERCOL through the development of new schemes for distributing panels on blade and hub surfaces. These include new methods for distributing panels over the blade span to replace the previous methods based on constant radius blade sections and provide improved panel shapes and flow resolution near the blade tips. The new panel distributions also allow inclusion of the effects of arbitrary axisymmetric hub shapes and filleting at the blade root.

AERCOL also developed a more robust iterative algorithm for enforcing a Kutta condition of zero pressure jump along blade trailing edges, and adapted part of the MIT lifting surface code PSF-2 (Greeley and Kerwin 1982) for use as a fast pre-processor in order to provide initial data for alignment of the pitch distribution of panels that form the near wakes of blades with the mean flow generated downstream of the propeller. In addition, lifting surface procedures developed at DREA for prediction of the speeds for inception of cavitation on blade surfaces were adapted for use in the surface panel code ASP-2.

This paper presents new results to supplement previously published cavitation inception correlations performed at DREA (Noble 1995). The previous results provided correlations of surface cavitation inception obtained with the steady, uniform inflow version of the code, named ASP-1, with model test data for one propeller and a range of advance coefficients in the open water condition. A correlation was provided as well with an ASP-2 prediction of cavitation inception at the blade root with full scale, sea trial data for one propeller and a single advance coefficient in a ship's wake. In this paper, ASP-2 predictions of inception of outer radius sheet cavitation on the blades of two propellers, and blade root cavitation on one propeller, are correlated with model test data over a range of advance coefficients in a ship's wake and with full scale data at the ship's normal operating condition.

THEORETICAL BACKGROUND

ASP-2 performs flow calculations in a frame of reference rotating with the propeller at constant angular rate Ω and advancing with the ship at constant forward speed V_s. The turbulent inflow entering the propeller disk due to upstream hull and appendage wake flows is approximated by a statistically time-averaged velocity distribution having radially and circumferentially varying axial, radial and tangential components relative to a ship-fixed cylindrical coordinate system with its origin at the propeller centre.

The assumptions of small circumferential variations of the axial inflow component and small magnitudes of transverse radial and tangential inflow components, relative to the circumferential-mean axial inflow velocity $V_a(r)$ at each radius, allow the integration of Euler's equation for fluid momentum conservation to obtain the following Bernoulli equation relating unsteady pressures and velocities at points on the propeller surface to corresponding mean flow values far upstream.

$$p + \frac{1}{2}\rho V_T^2 + \rho \frac{\partial \phi}{\partial t} = p_{atm} + \rho g (H - y_o) + \frac{1}{2}\rho U^2$$

Here, p and $V_T = \left| \vec{U} + \vec{\nabla}\phi \right|$ are the instantaneous total pressure and velocity at a point on the propeller surface, ρ is water density, ϕ is propeller-induced velocity potential, t is time, and g is the acceleration due to gravity. The propeller shaft centre is at a depth H below a free water surface at atmospheric pressure p_{atm}. At any time t measured relative to the time at which the blade is in its upward vertical position, variable y_o is the instantaneous upward vertical coordinate $r \cos(\theta - \Omega t)$ of a surface point at radius

r from the shaft centre and rotation plane angle θ from the blade's spanwise reference line. Velocity vector $\vec{U}$ is the mean relative inflow to a blade section at radius r, having a magnitude

$$U = \sqrt{V_a^2(r) + (r\Omega)^2}$$

From the preceding unsteady Bernoulli equation, a dimensionless pressure coefficient can be defined as

$$C_p = (p - p_{atm} - \rho g H) / (\tfrac{1}{2}\rho U^2) = C_p' - C_g$$

where the total pressure coefficient is broken into two terms, a flow-dependent term

$$C_p' = 1 - \left(\frac{V_T}{U}\right)^2 - \frac{2}{U^2}\frac{\partial \phi}{\partial t}$$

and a variable depth term due to blade rotation under gravity

$$C_g = 2 g y_o / U^2$$

For inviscid flows and a given inflow distribution, the pressure coefficient C_p' depends only on the propeller's advance coefficient, $J = V_s(1 - w_T)/(n D)$, where w_T is the Taylor wake fraction defined such that $V_s(1 - w_T)$ is the volumetric average of the axial inflow over the propeller disk, $n = \Omega / (2\pi)$ is shaft revolutions per second and D is propeller diameter.

If it can be assumed that the dimensionless ratios of statistically time-averaged inflow velocity to ship speed distributed over the propeller disk are essentially constant with increasing ship speed, then the following extrapolation formula for ship speed at cavitation inception at a point on the blade surface can be derived (Noble 1995) for any fixed advance coefficient J.

$$V_i = V_s \sqrt{(C_p^* + C_g) / C_p'}$$

In this equation, C_p^* is defined as a critical value of the total pressure coefficient C_p corresponding to the total pressure p equal to the vapour pressure of sea water p_v at cavitation inception, i.e.

$$C_p^* = (p_v - p_{atm} - \rho g H) / (\tfrac{1}{2}\rho U^2)$$

Since $C_p^* + C_g$ always evaluates to a negative number, the square root in the previous extrapolation formula for ship speed at cavitation inception is evaluated only at points on the blade surface where the flow-dependent pressure coefficient C_p' is negative.

For inception calculations, the pressure coefficients calculated by ASP-2 at surface panel control points are interpolated to a grid of fixed chord fractions along constant radius blade sections specified by the user, and a search is performed to find the minimum or most negative pressure coefficient on each side of constant radius sections over one revolution. The associated cavitation is then assumed to be of a sheet or bubble type depending on whether the section's inception point is located upstream or downstream of a prescribed chord station near the leading edge.

PROPELLERS AND INFLOW FIELDS

The two propellers examined in this paper will be designated as propellers A and B. Two-dimensional projected views of each propeller showing a single blade on its hub, and looking perpendicular and parallel to the propeller rotation plane, are provided in Figures 1 and 2.

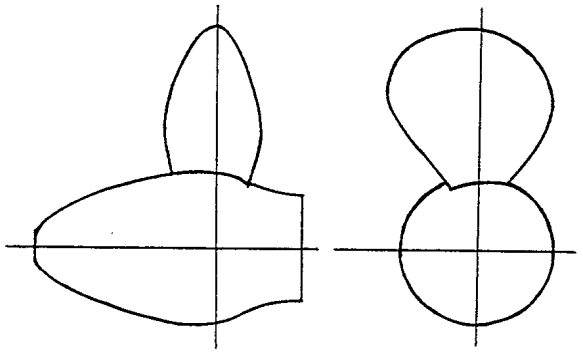

Figure 1: Projected Views of One Blade and Hub for Propeller A

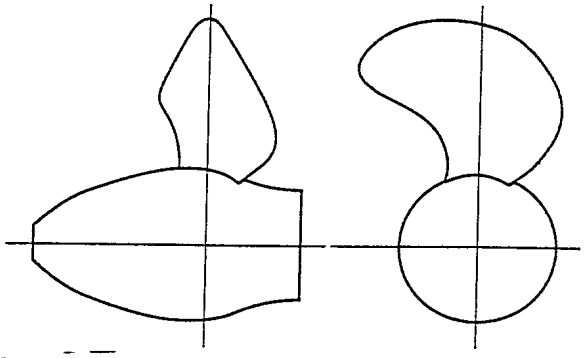

Figure 2: Projected Views of One Blade and Hub for Propeller B

These are five-bladed, controllable-pitch propellers that share the same large bulbous hub having a variable radius over the axial extent of its intersection with the blades. Like most propellers designed for improved cavitation performance, propeller B has blades with significant skew or downstream sweep.

In addition to propeller geometry, the distributions of the three components of statistically time-averaged inflow velocity incident on the propeller disk in a ship's wake are required as input to ASP-2. The propeller inflow fields used for cavitation performance predictions included in this paper were obtained from wake surveys performed by the Maritime Research Institute Netherlands (MARIN). Pitot tube measurements of nominal inflow velocities distributed over the port side propeller disk were made using a towed model of the twin-screw ship fitted with all appendages except for propellers. Typical axial, radial and tangential components of the nominal model wake velocity divided by ship speed entering the rotation plane of the right-handed, port side propeller examined here are plotted in Figure 3.

Following a convention of the International Towing Tank Conference, the axial inflow component is defined as being positive downstream parallel to the propeller shaft axis, the radial component is positive radially outward, and the tangential component is positive clockwise looking upstream. Velocities are plotted versus rotation plane angle measured relative to a downward vertical reference of zero degrees at various radius fractions or ratios of local radius to propeller tip radius over the propeller disk.

The axial component of inflow into the propeller planes of twin-screw vessels moving at constant speed on a straight course in flat calm seas has a slight radial and circumferential non-uniformity in the upper half of the propeller disk due to a combination of the flows generated by the upstream ship hull, propeller shafting and shaft support structures. From Figure 3, propeller blades are seen to cycle through about the same 20 percent axial flow deficit at all radius stations at blade position angles just beyond the top vertical angle of 180 degrees.

Small radial and tangential components of transverse inflow are present as well consisting mostly of a constant vertical velocity due to the slight inclination of the propeller shaft to the onset flow. Resolving a constant vertical velocity radially and tangentially produces radial and tangential components that follow a simple cosine and sine variation, respectively. Figure 3 shows deviations from this constant upwash particularly for the radial inflow component in the vicinity of the axial wake deficit.

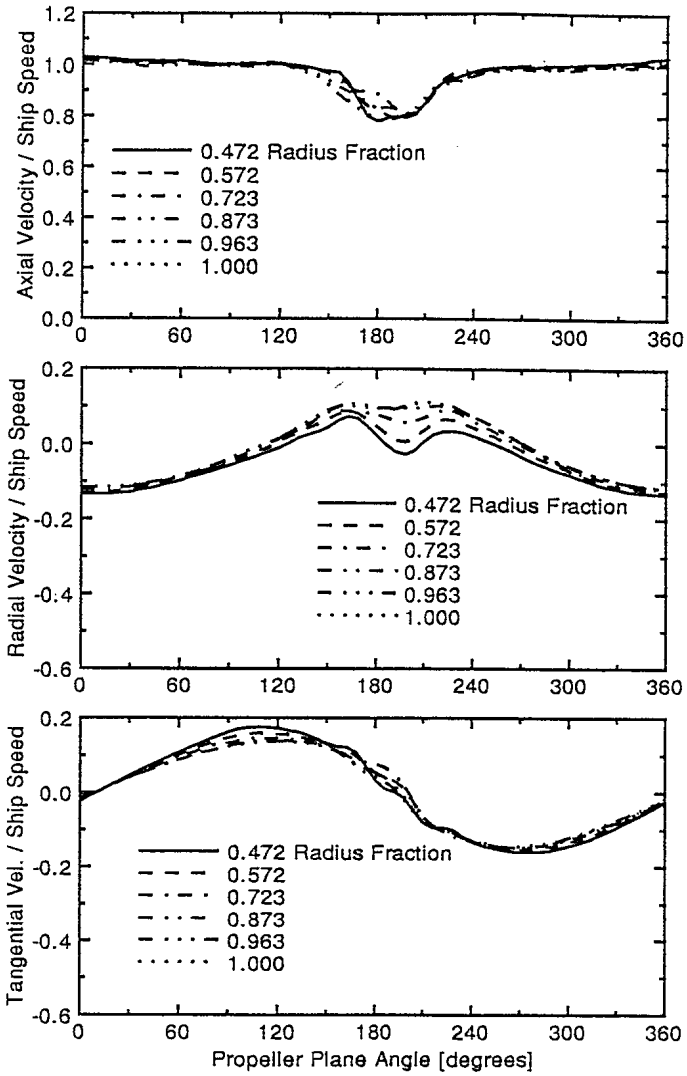

Figure 3: Propeller Inflow Velocities Input to ASP-2

SOLUTION PROCEDURES USED BY ASP-2

ASP-2, like its predecessor PUF-10, solves for a perturbation potential flow generated by the propeller that is a solution to Laplace's equation in terms of a perturbation velocity potential. Using one of Green's identities, the velocity potential can be expressed as the solution to an integral equation in terms of dipole and source singularity strengths distributed over the propeller surface and the surfaces of its downstream wake. For numerical solution, the integral equation is approximated by a system of linear algebraic equations by discretizing the propeller and wake surfaces into small quadrilateral panels or boundary elements with constant strength dipole and source singularities used on propeller panels, and dipole singularities on wake panels.

Curved, hyperboloidal-shaped panels are used on the propeller surface rather than flat panels to eliminate the effects of surface discontinuities between panels and improve the accuracy of solutions on the highly curved surfaces at blade extremities. To reduce the sensitivity of unsteady flow solutions to time step size, the first row of panels in the wakes of propeller blades use a linear or ramp dipole strength distribution rather than the constant strength dipoles used elsewhere.

The source strengths on the propeller surface panels are determined directly from relative inflow velocities by applying a flow tangency boundary condition of zero net flow velocity normal to the blade and hub surfaces. By the iterative enforcement of a Kutta condition of zero pressure jump along blade trailing edges and the implementation of a scheme for updating wake panel singularity strengths and vorticity shed into the wakes of blades as they rotate through the non-uniform inflow field, a system of linear equations is established for the unknown velocity potential at panel control points on propeller surfaces. The resulting perturbation flow velocity at control points is obtained directly from velocity potential by simple differentiation, and then the control point pressure is determined using the unsteady Bernoulli equation described earlier.

By assuming that all propeller blades have identical geometries and that propeller inflows are steady relative to a ship-fixed reference, the ASP-2 code and its predecessor PUF-10 reduce the computational effort by making use of this symmetry and solving for unknown potentials on only a single key blade and key hub segment passing between blades. The singularity strengths and influence of other blades and hub segments are then updated as they rotate and reach previous blade positions last calculated for the key blade and key hub segment.

ASP-2 first performs an initial steady flow solution that is identical on all blades and hub segments using the radially-varying, circumferential mean of the inflow field, and then the unsteady flow solution is obtained at a series of equally-spaced time steps or blade position angles as the blades are rotated through the circumferential inflow variations in a ship's wake. The unsteady solution continues for several revolutions until results on each blade have the same periodic variation at the shaft rotation rate.

For the present flow calculations, the edges of blade surface panels are distributed along lines running across the breadth of the blade using an algebraic, full-cosine spacing that concentrates panels near the blade's leading and trailing edges, and along lines running in a spanwise sense from root to tip using an equal arclength spacing. Hub segment panels passing between blades run from the constant radius shaft at a specified distance upstream of blade leading edges to the hub's downstream end. Hub panels are distributed axially and circumferentially using an elliptic gridding procedure that matches the spacing of the root-most panels on the blade or root fillet boundaries. The panels on the portion of the hub downstream of blade trailing edges are also aligned to the spacing of panels along the lowest radius boundaries of the initial mean-flow-aligned wake sheets representing the near wakes of propeller blades.

Based on a DREA evaluation of the convergence of steady flow solutions with increasing panel density obtained with ASP-1, the present unsteady flow results were obtained using a grid of 40 surface panels along grid lines running the breadth of each side of the key blade, and 35 panels along spanwise grid lines running from the hub to the blade tip. Additionally, the present calculations use 12 panels on the surface of the key hub segment distributed over an axial distance between the blade's leading edge and the location of a constant radius shaft upstream of the blades, and 12 circumferential panels distributed between the surfaces of adjacent blades.

CAVITATION INCEPTION PREDICTIONS

In this section of the paper, ASP-2 predictions for surface cavitation inception on the blades of propellers A and B are correlated with experimental results predicted at model scale for a range of advance coefficients in a ship's wake, and with sea trial observations at the normal operating advance coefficient of each propeller. The cavitation performance of the two propellers was examined at model scale by performing observations of propellers operating in the wake of a fully-appended ship model in MARIN's depressurized towing tank. Froude numbers and local cavitation numbers were matched to estimated full scale values, but Reynolds numbers were approximately an order of magnitude lower than the full scale flow condition.

To compensate for Reynolds number differences, MARIN artificially stimulated transitions to turbulent boundary layer flow near the leading edges of propeller blade sections using 60 μm roughness elements along the leading edges of the model's blades. An electrolysis source was used as well to generate sufficient cavitation nuclei in the propeller's inflow. MARIN has found these steps necessary to generate cavitation extents and inception speeds comparable to full scale observations.

DREA used its video propeller viewing system (Kennedy et al. 1989) to record the cavitation performance of propellers A and B during sea trials of surface ships moving at constant speed on a straight course under calm sea conditions. Inception points of the first types of cavitation to form on propeller B with

increasing ship speed were also confirmed acoustically using an acoustic sensor attached to the hull just above the propeller. This equipment was used to determine the inception speeds for cavitation forming near the leading edge of outer radius blade sections of propellers A and B, and on the root-most sections of the blades of propeller B.

For correlations of cavitation inception predictions with experiment in this section, inception speed results have been non-dimensionalized by defining a local cavitation number

$$\sigma_n = (p_{atm} + \rho g H - p_v) / (\tfrac{1}{2}\rho n_i^2 D^2)$$

where n_i is shaft revolutions per second at inception defined by ASP-2 from the inception ship speed V_i and advance coefficient as $n_i = V_i(1 - w_T) / (JD)$.

Figures 4 and 5 show correlations of local cavitation number versus advance coefficient for sheet cavitation forming near blade leading edges on both the back (or upstream) surface and the face (or downstream) surface at outer radius sections of propeller A. Correlations were made with blades at their design pitch setting. Full scale sea trial results were obtained at advance coefficient $J = 0.98$, and showed significant blade-to-blade variations in inception speeds. These results are plotted in the figures as a range of values observed over all blades. Experimental data for inception of blade root cavitation are not available for Propeller A.

Figure 4 shows a good correlation of ASP-2 predictions of the inception of back sheet cavitation on propeller A with MARIN's model test data over the complete range of advance coefficient. ASP-2 and model test predictions have slightly higher cavitation numbers or lower inception speeds than the sea trial observations made at the operating advance coefficient. ASP-2 predicts inception of back sheet cavitation at a chord fraction of 0.018 and radius fraction of 0.95 just past the top vertical blade position, which is in agreement with the general location observed at model and full scale.

In contrast, the correlation presented in Figure 5 shows ASP-2 predictions of inception of outer radius face sheet cavitation to be significantly different than model test results. The ASP-2 prediction of higher cavitation numbers or lower inception speeds than the model test is in much better agreement with the sea trial observation at $J = 0.98$. Inception of face sheet cavitation is predicted by ASP-2 at a chord fraction of 0.006 and radius fraction of 0.87 with the blade nearly horizontal and coming up to the top vertical position, which again is close to observations at both model and full scale.

Table 1 summarizes the correlations of ASP-2 predictions of normalized ship speeds for sheet cavitation inception on Propeller A with both model test and sea trial observations at the operating advance coefficient. In this table, ship speeds at inception have been divided by the lowest speed observed for each type of cavitation on the sea trial. ASP-2 and model test predictions are 3 to 5 percent lower than the lowest sea trial speed observed for back sheet cavitation. On the other hand, the model test result for face sheet cavitation is 56 percent higher than the lowest sea trial speed and falls significantly outside the range of sea trial observations. ASP-2's prediction is only 10 percent higher than the lowest sea trial speed and falls within the range observed for trialed blades.

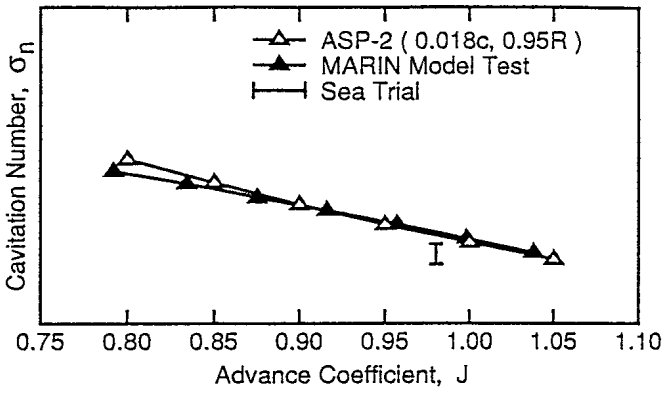

Figure 4: Outer Radius Back Sheet Cavitation Inception for Propeller A

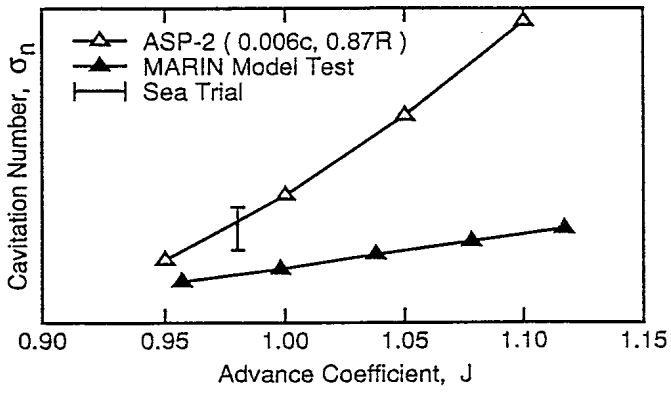

Figure 5: Outer Radius Face Sheet Cavitation Inception for Propeller A

Type	Model	ASP-2	Sea Trial
Back Sheet	0.95	0.97	1.00 - 1.18
Face Sheet	1.56	1.10	1.00 - 1.23

Table 1: Normalized Inception Speeds for Propeller A at $J = 0.98$

Figures 6 to 8 show correlations for Propeller B of local cavitation number versus advance coefficient of outer radius back sheet cavitation, as well as back and face cavitation forming at the blade roots. Outer radius face sheet cavitation is not a problem for this propeller. Correlations are again made with the blades at their design pitch setting. The sea trial results were obtained over a range of advance coefficient from J = 1.04 to 1.10 as the various types of cavitation formed in different speed ranges along the ship's operating curve. As for Propeller A, the sea trial results obtained with Propeller B showed significant blade-to-blade variations in inception speed and are plotted in figures as a range of values observed over all blades for each type of cavitation.

Figure 6 shows a good correlation of ASP-2 results for inception of back sheet cavitation on propeller B with MARIN's model test data, particularly in the upper range of advance coefficient close to the normal operating condition. ASP-2 and model tests have a slightly lower cavitation number or higher inception speed than the sea trial observation made at J = 1.05. Over the range of advance coefficient, ASP-2 predicts inception of back sheet cavitation at chord fractions varying from 0.012 to 0.018 and at radius fractions varying from 0.85 to 0.95. The back sheet cavitation occurred at blade positions just past the top vertical which agrees with both model and full scale observations.

Figure 7 compares results for midchord bubble cavitation forming at the blade roots on the back surface of Propeller B. ASP-2 in seen to overpredict the sea trial observations made at J = 1.04, while model tests are seen to underpredict sea trial results. The differences could be due to viscous flow effects at the blade root that may either generate flow separation or produce a juncture vortex that affects results in the midchord region, with MARIN's model tests conducted at too low a Reynolds number and ASP-2 not modelling these effects at all.

Correlations of results for root cavitation forming near the leading edges on the face or downstream surface of the blades of Propeller B are provided in Figure 8. ASP-2 predictions are at much higher cavitation numbers or much lower inception speeds than are observed at model scale, but are seen to fall within the range of variations observed at full scale at an advance coefficient close to 1.1. For face root cavitation forming near the blade leading edges, the effects of the lower Reynolds number in model tests appear to be much greater than the effects of potential flow assumptions used in ASP-2.

Table 2 summarizes results obtained for correlations of ASP-2 predictions of normalized inception speeds with both model test and sea trial observations for Propeller B. Inception speeds are again divided by the lowest speed observed for each type of cavitation on the sea trial.

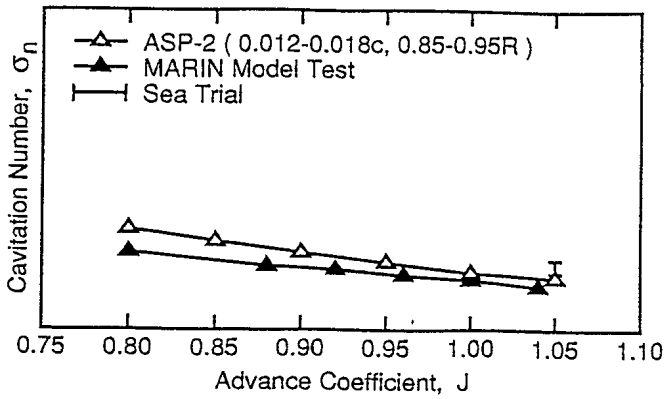

Figure 6: Outer Radius Back Sheet Cavitation Inception for Propeller B

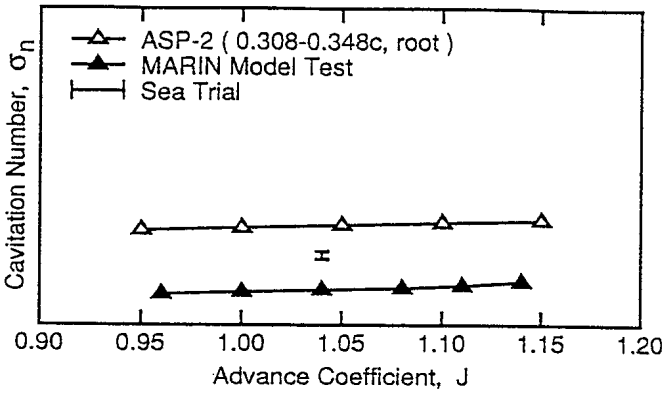

Figure 7: Midchord Back Root Cavitation Inception for Propeller B

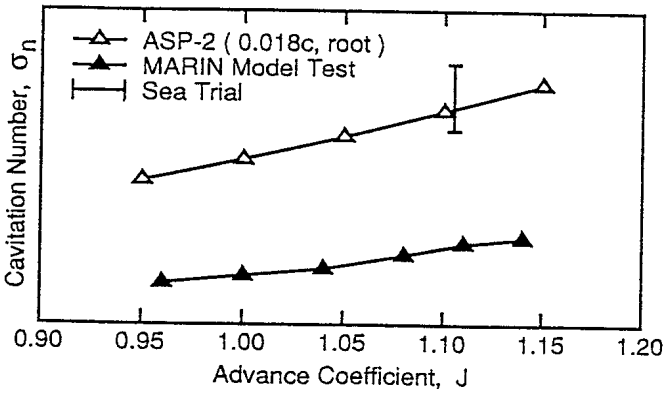

Figure 8: Leading Edge Face Root Cavitation Inception for Propeller B

Type	J	Model	ASP-2	Sea Trial
Back Sheet	1.05	1.25	1.15	1.00 - 1.10
Back Root	1.04	1.49	0.90	1.00 - 1.11
Face Root	1.10	1.72	1.14	1.00 - 1.16

Table 2: Normalized Inception Speeds for Propeller B

From Table 2, ASP-2 and model tests are seen to overpredict the lowest inception speed for back sheet cavitation observed on sea trials by 15 and 25 percent, respectively, with ASP-2 only 5 percent higher and the model test 15 percent higher than the highest speed observed on trialed blades. While ASP-2 and model tests fall on opposite sides of sea trial results for midchord back bubble cavitation at the blade root, ASP-2 is only 10 percent lower than the lowest sea trial speed while model tests are 38 percent higher than the highest sea trial speed. Finally, for leading edge face cavitation at the blade root, the ASP-2 prediction falls within the 16 percent blade-to-blade variation observed for trialed blades, while the model test prediction is over 70 percent higher than the lowest sea trial speed.

CONCLUDING REMARKS

This paper has described the propeller surface panel code ASP-2 developed for DREA by Canadian contractor AERCOL that can be used to predict the inception of surface cavitation forming on the blades of marine propellers operating in a ship's wake. Comparisons of ASP-2 predictions of cavitation inception performance of two propellers are made with both model test data over a wide range of advance coefficient and with sea trial data at normal operating conditions.

ASP-2 and MARIN's model test predictions of outer radius back sheet cavitation for each propeller agree well over a wide range of advance coefficient, and both are reasonably close to sea trial observations at operating advance coefficients. In contrast, ASP-2's predictions of speeds for inception of outer radius face sheet cavitation on one propeller are significantly lower than model test results over the complete range of advance coefficient examined, but are in much better agreement with the sea trial data at normal operating conditions.

Effects of Reynolds number appear to be evident in the results obtained for blade root cavitation on one propeller. While ASP-2's potential flow calculations and MARIN's model test results for midchord bubble cavitation at the blade root are on opposite sides of the sea trial data, the model test inception speeds are somewhat further from the range of speeds observed in sea trials. ASP-2's prediction of speeds for inception of face cavitation forming near the leading edge at the blade root falls within the range of sea trial data, while MARIN's model tests greatly overpredict the range of full scale inception speeds.

The good correlations of ASP-2 predictions with full scale sea trial observations demonstrate the code's ability to predict the performance of leading edge cavitation on both outer radius and root sections of propeller blades. The predictions of leading edge cavitation are close enough to full scale observations that the code can be used as a cost-effective tool for optimizing the inception performance of this type of cavitation in new propeller designs, and for examining remedies to leading edge cavitation problems that may arise with existing propellers. Development of viscous flow solvers will likely be necessary to improve predictions of midchord bubble cavitation and include effects of juncture vortices and flow separation at the blade roots.

REFERENCES

Greeley, D.S. and Kerwin, J.E., 1982, "Numerical Methods for Propeller Design and Analysis in Steady Flow," Trans. SNAME , Vol. 90, pp. 415-453.

Hsin, C.-Y., 1990, "Development and Analysis of Panel Methods for Propellers in Unsteady Flow," Ph. D. Thesis, Dept. of Ocean Engineering, MIT.

Kennedy, J.L., Sponagle, N.C., Wheaton, D.W., MacDonald, P. and Creaser, R.W., 1989, "Video Systems for Propeller Viewing," Proceedings of the 22nd ATTC, St. John's, Nfld.

Noble, D.J., 1995, "Numerical Prediction of the Cavitation Inception Performance of Marine Propellers," Proc. of the Third Canadian Marine Hydrodynamics and Structures Conference, Halifax/Dartmouth, Nova Scotia.

#503805